# Fidelity in topological quantum phases of matter

Silvano Garnerone,* Damian Abasto, Stephan Haas, and Paolo Zanardi†
*Department of Physics and Astronomy, Center for Quantum Information Science and Technology, University of Southern California, Los Angeles, California 90089, USA*
(Received 23 January 2009; published 4 March 2009)

Quantum phase transitions that take place between two distinct topological phases remain an unexplored area for the applicability of the fidelity approach. Here, we apply this method to spin systems in two and three dimensions and show that the fidelity susceptibility can be used to determine the boundary between different topological phases particular to these models, while at the same time offer information about the critical exponent of the correlation length. The success of this approach relies on its independence on local-order parameters or breaking symmetry mechanisms, with which nontopological phases are usually characterized. We also consider a topological insulator-superconducting phase transition in three dimensions and point out the relevant features of fidelity susceptibility at the boundary between these phases.

DOI: 10.1103/PhysRevA.79.032302 PACS number(s): 03.67.−a, 64.70.Tg, 24.10.Cn

## I. INTRODUCTION

In recent years topological phases have been intensively studied in condensed-matter systems. These exotic states appear in different contexts, such as fractional quantum Hall physics, spin liquids, and topological insulators [1–7]. Their understanding is relevant to topological quantum computation, which provides the paradigm to store and manipulate information in topologically nontrivial systems [8]. In a seminal work [3] Kitaev introduced a spin model which can be exactly solved using a mapping to Majorana fermions coupled to a static $\mathbb{Z}_2$ gauge field [9] (see also Ref. [10] for a perturbative approach). Generalizations of the Kitaev model with respect to lattice geometry, spatial dimension, and local Hilbert-space dimension have appeared recently [6,11,12]. In some regions of parameter space these models have nontrivial topological properties which cannot be described by any local-order parameter. This prevents the direct applicability of the Landau-Ginzburg paradigm for the study of their phase transitions. Alternative ways of understanding criticality in systems with no local-order parameter have been suggested in connection to quantum information. In particular, entanglement entropy (for a review, see Ref. [13]) and the fidelity approach [14–18] have attracted a lot of attention (for a review, see Ref. [19]). The reason why these two quantities can describe topological phases or determine their boundaries is due to the fact that they depend only on the properties of the ground state of the system and do not require *a priori* knowledge of any order parameter.

In this paper we shall focus on the fidelity approach to topological phase transitions [20–22]. Much work has been done in understanding the nature of the phases in the Kitaev honeycomb model and, in particular, its fidelity has been studied in Refs. [23,24]. The present work aims to provide a more general understanding of fidelity in topological phase transitions. For this purpose we consider two- and three-dimensional (3D) extensions of the Kitaev honeycomb model. The models we chose differ from Kitaev's model in the geometry of the lattice and the interactions or the dimension of the ambient space and of the local Hilbert space.

## II. MODELS AND METHOD

The dramatic changes in a many-body ground state $|\Psi_0(\lambda)\rangle$ across a quantum phase transition can be captured by the fidelity $F=|\langle\Psi_0(\lambda)|\Psi_0(\lambda+\delta\lambda)\rangle|$ between two ground states corresponding to slightly different values of the set of parameters defining the Hamiltonian $H(\{\lambda\})$. Alternatively, one can use the fidelity susceptibility $\chi=\lim_{\delta\lambda\to 0}\frac{-2\ln F}{\delta\lambda^2}$ [25]. The fidelity quantifies how different two quantum states are. Given the drastic changes that take place across a quantum phase transition, one should expect the fidelity for nearby states to exhibit a drop across the boundary phase, signaling an enhanced distinguishability. Indeed, while in the thermodynamic limit the fidelity (susceptibility) has a drop (divergence) at the quantum critical point, for finite-size systems this behavior is translated in the fidelity susceptibility being extensive away from criticality, while superextensive at criticality when the operator driving the transition is sufficiently relevant [18]. Moreover, a scaling analysis of the fidelity susceptibility can be performed to extract the critical exponent $\nu$ of the correlation length $\xi$.

Here we apply this tool from quantum information theory to study the quantum phase transition between two distinct topological phases in three models: mosaic models, Kitaev's honeycomb model with an external magnetic field, and a 3D model exhibiting a transition between two distinct non-Abelian topological phases. Let us first review them very briefly.

An elegant way to look at the Kitaev model as a special instance of a more general class of models is provided by the mosaic classification [1]. Mosaic models are defined on two-dimensional Bravais lattices constructed with a trivalent vertex building block, constrained by translational and rotational symmetries. The trivalent vertex is the local border between three polygons (see Fig. 1). The number of edges of the three polygons $(e_1,e_2,e_3)$ specifies the mosaic model and

*garneron@usc.edu
†Also at Institute for Scientific Interchange, Viale Settimio Severo 65, I-10133 Torino, Italy.

 

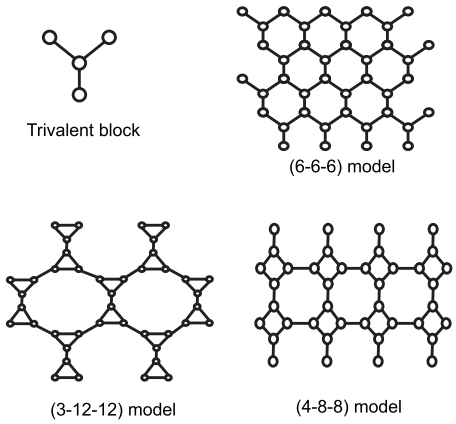


FIG. 1. The trivalent vertex and the three different mosaic models constructed with it, which are considered in the present work.

only four possible such lattices are allowed: (6-6-6), corresponding to the Kitaev model; (3-12-12), corresponding to the model studied in [6]; (4-6-12); and (4-8-8).

The Hamiltonian of all mosaic spin models is given by

$$H = -\sum_{u=x,y,z} J_u \sum_{(i,j)\in S(u)} \sigma_i^u \sigma_j^u, \tag{1}$$

where $S(u)$ is the set of edges in the $u$ direction. At every site the Hilbert space associated with the spin-1/2 particle is identified with a two-dimensional physical subspace $\mathcal{M}$ of a four-dimensional Fock space $\tilde{\mathcal{M}}$, introduced to solve the model. The Pauli operators acting on $\mathcal{M}$ are represented by four Majorana operators on $\tilde{\mathcal{M}}$: $\sigma^x = ib^x c$, $\sigma^y = ib^y c$, and $\sigma^z = ib^z c$ with $\alpha^2 = 1$ and $\alpha\beta = -\beta\alpha$, for $\alpha, \beta \in \{b^x, b^y, b^z, c\}$, and $\alpha \neq \beta$. The physical subspace is obtained through a projection $|\psi\rangle \in \mathcal{M} \Leftrightarrow D|\psi\rangle = |\psi\rangle$ with $D = ib^x b^y b^z c$. The Hamiltonian (1) can be rewritten as $H = \frac{1}{2}\Sigma_{i,j} \hat{A}_{i,j} c_i c_j$ with the operators $\hat{A}_{ij} = iJ_u \hat{Z}_{ij}$, where $\hat{Z}_{ij} = ib_i^u b_j^u$ and $(i,j) \in S(u)$ ($\hat{A}_{ij} = 0$ otherwise). The operators $\hat{Z}_{ij}$ commute with each other and with the Hamiltonian, so the space of the multispin system $\mathcal{L}$ can be decomposed as a direct sum $\mathcal{L} = \oplus_Z \mathcal{L}_Z$, where each sector is indexed by a set of eigenvalues $\{z_{ij} = \pm 1 | (i,j) \in S(u), u = x,y,z\}$ of the operator $\hat{Z}_{ij}$. Within each sector, the Hamiltonian reduces to a quadratic form in the Majorana operators $c_i$. The couplings of the Hamiltonian depend on a choice of vortex configuration, given by the eigenvalues of the plaquette operators $W_{p(n_i)} = -\Pi_{i,j\in\partial p(n_i)} Z_{ij}$, one for each of the $n_i$ isogons [$\partial p(n_i)$ is the set of links belonging to plaquette $p(n_i)$]. The operators $W_{p(n_i)}$ commute with each other and with the Hamiltonian and since $W_{p(n_i)}^2 = 1$, their eigenvalues are $w_p = \pm 1$. A plaquette with $w_p = +1$ is a vortex-free plaquette, while $w_p = -1$ corresponds to a vortex. In the following, we restrict ourselves to the vortex-free sector, with a choice of $z_{ij}$ that preserves translational symmetry. The ground-state energy is at a minimum for this configuration [26].

Another modification of the Kitaev model that preserves its topological nature is the addition of a three-spin interaction of the form

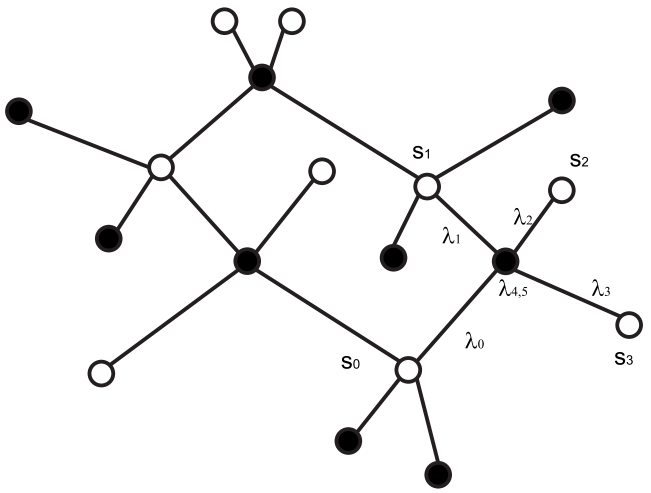


FIG. 2. The diamond lattice used in the three-dimensional extension of the Kitaev model.

$$H = -\sum_{u=x,y,z} J_u \sum_{(i,j)\in S(u)} \sigma_i^u \sigma_j^u - K \sum_{i,j,k} \sigma_i^x \sigma_j^y \sigma_k^z, \tag{2}$$

where the $K$ term is obtained through a perturbative expansion of a weak (Zeeman) magnetic field $V = \mathbf{h}\cdot\sigma$ [27]. In this case $K \sim \frac{h_x h_y h_z}{J^2}$ and this Hamiltonian is assumed to approximate the one with a Zeeman term when $K \ll J$ with $J_u = J$. The inclusion of this magnetic perturbation to the original model generates a topological phase with non-Abelian anyonic excitations in the regime $|J_z| \leq |J_x| + |J_y|, |J_y| \leq |J_z| + |J_x|, |J_x| \leq |J_y| + |J_z|$, while outside this region the excitations remain Abelian.

Recently analogs of the Kitaev model on three-dimensional lattices have been constructed [11,28]. In the present work we focus on the model introduced in Ref. [11] since it presents quantum phase transitions between distinct nontrivial topological phases that, to our knowledge, have never been investigated with the fidelity approach. The model is defined on a diamond lattice and has a four-dimensional local Hilbert space (see Fig. 2). The Hamiltonian is the following:

$$H = -\sum_{u=0}^{3} J_u \sum_{(i,j)\in S(u)} \sigma_j^u \sigma_k^u (\tau_j^x \tau_k^x + \tau_j^z \tau_k^z), \tag{3}$$

where $\sigma$ and $\tau$ are Pauli spin matrices associated to the two local spin-1/2 degree of freedoms at each point in the lattice. As shown in [11] Hamiltonian (3) can be mapped to a free Majorana Hamiltonian which, in its ground-state sector, is given by

$$H = i\sum_{u=0}^{3} J_u \sum_{(i,j)\in S(u)} (\lambda_j^4 \lambda_k^4 + \lambda_j^5 \lambda_k^5) \tag{4}$$

and $\lambda_i^{4,5}$ are Majorana fermions introduced in the representation of the Pauli spin matrices (see Ref. [11] for details), analogous to the previous model Hamiltonians. The addition of next-nearest-neighbor interactions into Eq. (4) allows for the presence of distinct nontrivial topological phases in the phase diagram, as we shall see in Sec. III.

The spin realization of all the above models can be mapped onto a free Majorana fermion Hamiltonian

$$H(A) = \frac{i}{4}\sum_{i,j} A_{i,j} c_i c_j, \tag{5}$$

where $A_{i,j}$ encodes the lattice structure and the parameters of the model. Once a unit cell of size $s$ has been chosen the Hamiltonian can be written in direct space as

$$H(A) = \frac{i}{4}\sum_{n,\nu;m,\mu} A_{n,\nu;m,\mu} c_{n,\nu} c_{m,\mu}, \tag{6}$$

where $n$ and $m$ are the positions of the unit cells in the lattice and $\mu$ and $\nu$ are the positions of the vertices inside the unit cell. Due to translational invariance $A$ depends only on $\nu$, $\mu$, and $m-n$. Using a Fourier transform, we obtain

$$H = \sum_{\mathbf{k}} \mathbf{\Psi}^\dagger(\mathbf{k}) \mathcal{H}(\mathbf{k}) \mathbf{\Psi}(\mathbf{k}) \tag{7}$$

with $\Psi_\alpha(\mathbf{k}) = (1/\sqrt{N})\Sigma_{\mathbf{r}} e^{-i\mathbf{k}\cdot\mathbf{r}} c_{\mathbf{r},\alpha}$ as a complex fermion, $N = sL^d$ as the system size, $L$ as the number of unit cells in one direction of the $d$-dimensional lattice, and $s$ as the size of the unit cell with $\alpha \in \{1,2,..,s\}$. Then in general we have to deal with a free-fermion model characterized by $s$ different bands. The ground state is obtained filling the Fermi sea, where all the levels with negative energy $\epsilon_\beta(\mathbf{k}) < 0$ are occupied,

$$|\Psi_0\rangle \equiv \prod_{\beta,\mathbf{k}} b^\dagger_\beta(\mathbf{k})|0\rangle, \tag{8}$$

if $\epsilon_\beta(\mathbf{k}) < 0$. $b^\dagger_\beta(\mathbf{k}) \equiv \mathbf{\Psi}^\dagger(\mathbf{k}) \cdot \mathbf{V}_\beta(\mathbf{k})$, where $\mathbf{V}_\beta(\mathbf{k})$ is the eigenvector associated to the $\epsilon_\beta(\mathbf{k})$ eigenvalue of $\mathcal{H}(\mathbf{k})$. The matrix $U(\mathbf{k})$ diagonalizing $\mathcal{H}(\mathbf{k})$ has as column vectors $V_\beta(\mathbf{k})$. The spectrum of the single-body Hamiltonian $\mathcal{H}(\mathbf{k})$ is symmetric around zero.

The $\mathbf{k}$ component of the many-body ground state $|\Psi_0\rangle = \Pi_{\mathbf{k}} |\Psi_0\rangle_{\mathbf{k}}$ in first quantization is given by a functional Slater determinant. The $j$th component of the eigenstate corresponding to the $\beta$th band is represented by $V_{j,\beta}(\mathbf{k})$. Denoting with $s_n$ the number of negative single-particle energy bands, the first quantized wave function at fixed $\mathbf{k}$ is the Slater determinant of $s_n$ particles that can occupy $s_n$ bands,

$$\langle j_1, \ldots, j_{s_n} | \Psi_0 \rangle_{\mathbf{k}} = \frac{1}{\sqrt{s_n!}} \begin{vmatrix} V_{j_1,1}(\mathbf{k}) & \cdots & V_{j_1,s_n}(\mathbf{k}) \\ \vdots & \ddots & \vdots \\ V_{j_{s_n},1}(\mathbf{k}) & \cdots & V_{j_{s_n},s_n}(\mathbf{k}) \end{vmatrix} \tag{9}$$

with $j_i \in \{1,2,\ldots,s\}$. For these particular models, the fidelity corresponds to the product over all $\mathbf{k}$ of the absolute value of the overlap of two Slater determinants at different parameter values $\|\langle \tilde{\Psi}_0 | \Psi_0 \rangle\| = \otimes_{\mathbf{k}} \|\langle \tilde{\Psi}_0 | \Psi_0 \rangle\|_{\mathbf{k}}$ with

$$\langle \tilde{\Psi}_0 | \Psi_0 \rangle_{\mathbf{k}} = \frac{1}{s_n!} \sum_{j_1,\ldots,j_{s_n}} \begin{vmatrix} \tilde{V}_{j_1,1}(\mathbf{k}) & \cdots & \tilde{V}_{j_1,s_n}(\mathbf{k}) \\ \vdots & \ddots & \vdots \\ \tilde{V}_{j_{s_n},1}(\mathbf{k}) & \cdots & \tilde{V}_{j_{s_n},s_n}(\mathbf{k}) \end{vmatrix}^* \times \begin{vmatrix} V_{j_1,1}(\mathbf{k}) & \cdots & V_{j_1,s_n}(\mathbf{k}) \\ \vdots & \ddots & \vdots \\ V_{j_{s_n},1}(\mathbf{k}) & \cdots & V_{j_{s_n},s_n}(\mathbf{k}) \end{vmatrix}. \tag{10}$$

The previous expression, using the properties of determinants, can be rewritten as (for a proof, see p. 291 of Ref. [29])

$$\begin{vmatrix} \tilde{\mathbf{V}}^*_1(\mathbf{k}) \cdot \mathbf{V}_1(\mathbf{k}) & \cdots & \tilde{\mathbf{V}}^*_1(\mathbf{k}) \cdot \mathbf{V}_{s_n}(\mathbf{k}) \\ \vdots & \ddots & \vdots \\ \tilde{\mathbf{V}}^*_{s_n}(\mathbf{k}) \cdot \mathbf{V}_1(\mathbf{k}) & \cdots & \tilde{\mathbf{V}}^*_{s_n}(\mathbf{k}) \cdot \mathbf{V}_{s_n}(\mathbf{k}) \end{vmatrix}. \tag{11}$$

The above formula will be used in the evaluation of fidelity for the models that we consider.

## III. RESULTS

In this section we study how the fidelity susceptibility behaves for the mosaic models (4-8-8) and (3-12-12), for model (2), and for the three-dimensional Kitaev model (3).

### A. Mosaic models

Let us first focus on the (4-8-8) mosaic model [30]. Choosing a four-site unit cell, a Fourier transform of the Hamiltonian gives

$$H = \frac{1}{2}\sum_{\mathbf{k}} \mathbf{\Psi}^\dagger(\mathbf{k}) \mathcal{H}(\mathbf{k}) \mathbf{\Psi}(\mathbf{k}), \tag{12}$$

where

$$\mathcal{H}(\mathbf{k}) = \begin{pmatrix} J_x \sigma^y & -iJ_y \sigma^x + iJ_z \alpha \\ iJ_y \sigma^x - iJ_z \alpha^\dagger & J_x \sigma^y \end{pmatrix}, \tag{13}$$

$\Psi^\dagger_{\mathbf{k}} = (a^\dagger_{\mathbf{k},1}, a^\dagger_{\mathbf{k},2}, a^\dagger_{\mathbf{k},3}, a^\dagger_{\mathbf{k},4})$ is the Fourier transform of the Majorana operators $\{\Psi_i\}_{i=1}^4$, $\alpha = \mathrm{diag}[\exp(-ik_2), -\exp(ik_1)]$, $k_1 = \mathbf{k}\cdot\mathbf{n}_1$, $k_2 = \mathbf{k}\cdot\mathbf{n}_2$, $\mathbf{n}_1 = (1,0)$, and $\mathbf{n}_2 = (0,1)$. The system size is $N = 2L^2$. This model presents a quantum phase transition between two gapped phases with Abelian anyons when $J_z^2 = J_x^2 + J_y^2$. The phases are algebraically distinct, although they can be related by rotational symmetry.

For the (3-12-12) mosaic model [6,31], a Fourier transform with a six-unit cell renders the Hamiltonian in the form

$$\begin{aligned} H = \frac{i}{2}(&- a^\dagger_{\mathbf{k},1} a_{\mathbf{k},2} - a^\dagger_{\mathbf{k},1} a_{\mathbf{k},3} + J e^{-i\mathbf{k}\cdot\mathbf{n}_1} a^\dagger_{\mathbf{k},1} a_{\mathbf{k},2} + a^\dagger_{\mathbf{k},2} a_{\mathbf{k},3} \\ &- J e^{i\mathbf{k}\cdot\mathbf{n}_2} a^\dagger_{\mathbf{k},1} a_{\mathbf{k},2} - J a^\dagger_{\mathbf{k},3} a_{\mathbf{k},6} - a^\dagger_{\mathbf{k},4} a_{\mathbf{k},5} - a^\dagger_{\mathbf{k},4} a_{\mathbf{k},6} \\ &- a^\dagger_{\mathbf{k},5} a_{\mathbf{k},6}) + \mathrm{H.c.} \end{aligned} \tag{14}$$

with $\mathbf{n}_1 = (1/2, \sqrt{3}/2)$ and $\mathbf{n}_2 = (1/2, -\sqrt{3}/2)$. The single-particle Hamiltonian $A(\mathbf{k})$ is $6\times 6$ and the system size is

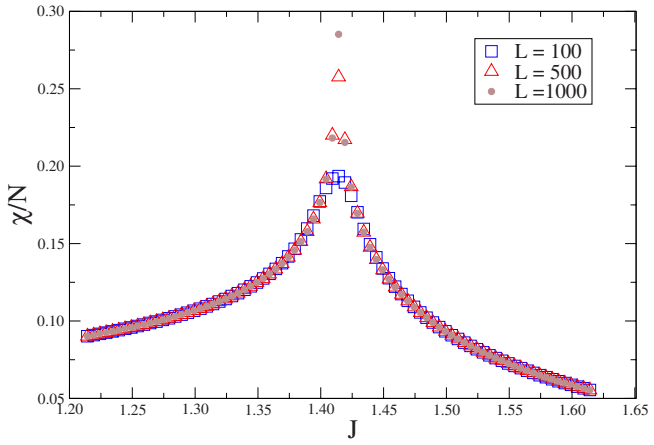


FIG. 3. (Color online) Fidelity susceptibility $\chi$ per site for the (4-8-8) mosaic model around the quantum critical point $J_z=\sqrt{2}$, separating two topological phases ($J_x=J_y=1$). $\chi$ shows extensive behavior off criticality, while it is superextensive at the critical point.

$N=6L^2$. This system has a quantum phase transition at $J=\sqrt{3}$ from a topological phase with Abelian anyons to one with non-Abelian anyons, spontaneously breaking time-reversal symmetry, without the need of an external magnetic field.

The numerical results for the fidelity susceptibility $\chi=\lim_{\delta\lambda\to 0}-2\ln F/\delta\lambda^2$ for the (4-8-8) mosaic model are shown in Fig. 3 for different system sizes, taking $J_x=J_y=1, J_z\in(1.21,1.61)$. We see that $\chi$ is an extensive quantity off criticality, while it is superextensive at the critical point $J_z^c=\sqrt{2}$.

We perform finite-size scaling for the susceptibility around the critical point $J_z^c=\sqrt{2}$. For a finite sample size we denote the point at which $\chi$ is maximum as $\chi^{\max}$, evaluated at $J_z=J_z^{\max}$. It scales as $\chi^{\max}/N\propto L^{\mu}$ with $\mu>0$, while in the thermodynamic limit $\chi/N\propto 1/|J'-J_z^c|^{\alpha}$. In Fig. 4(a) we plot $\log\chi^{\max}$ vs $\log L$ for system sizes $L\in[300,1000]$ in steps of 100 with $\delta J=10^{-6}$. We obtain that $\chi^{\max}/N\simeq L^{\mu}$ with $\mu=0.1523\pm0.0001$. (b) Data collapse for the fidelity susceptibility around the critical point $J_z^c=\sqrt{2}$. All curves collapse when plotted as a function of the dimensionless quantity $L^{1/\nu}(J_z-J_z^{\max})/J_z^c$ with critical exponent $\nu=1.105\pm0.070$.

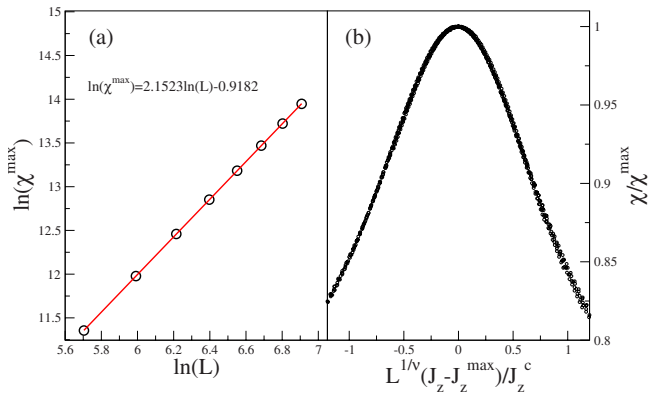


FIG. 4. (Color online) (a) Scaling analysis of the fidelity susceptibility at criticality for the (4-8-8) mosaic model for system sizes $L\in[300,1000]$ in steps of 100 with $\delta J=10^{-6}$. We obtain that $\chi^{\max}/N\simeq L^{\mu}$ with $\mu=0.1523\pm0.0001$. (b) Data collapse for the fidelity susceptibility around the critical point $J_z^c=\sqrt{2}$. All curves collapse when plotted as a function of the dimensionless quantity $L^{1/\nu}(J_z-J_z^{\max})/J_z^c$ with critical exponent $\nu=1.105\pm0.070$.

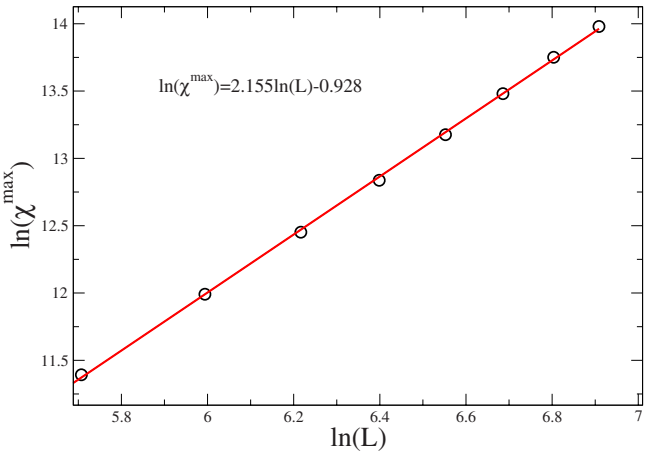


FIG. 5. (Color online) Scaling analysis of the susceptibility at criticality for the (3-12-12) mosaic model for $L\in[301,1001]$ in steps of 100. The fidelity signals the quantum phase transition separating the two distinct topological phases at $J=\sqrt{3}$, behaving as $\chi^{\max}/N\simeq L^{\mu}$ with $\mu=0.155\pm0.009$.

100 with $\delta J=10^{-6}$. We obtain superextensive scaling given by $\mu=0.1523\pm0.0001$.

Furthermore, we perform a data collapse, using the scaling ansatz [32],

$$\frac{\chi(J)}{\chi^{\max}}\simeq f\left(\frac{J_z-J_z^{\max}}{\sqrt{2}}L^{1/\nu}\right). \tag{15}$$

To quantify the extent of the collapse, we use a method similar to the one described in Ref. [33], obtaining the value $\nu=1.105\pm0.07$. From there, we conclude that $\alpha=\frac{\mu}{\nu}=0.138\pm0.009$. The result for the data collapse is shown in Fig. 4(b).

A similar analysis has been performed for the (3-12-12) mosaic model [6], confirming that the fidelity is superextensive at criticality with $\mu=0.155\pm0.009$ as seen on Fig. 5. However, we have not been able to obtain a satisfactory data collapse for the (3-12-12) mosaic model, probably due to numerical errors.

### B. Kitaev model with three-spin interaction

This model can be exactly diagonalized using the techniques we have summarized above. In particular, the Hamiltonian in Eq. (2) takes the form $H=\frac{1}{2}\Sigma_{i,j}\hat{A}_{i,j}c_ic_j$ with $\hat{A}_{ij}=iJ_u\hat{Z}_{ij}+K\Sigma_k\hat{Z}_{ik}\hat{Z}_{jk}$, and for the vortex-free case, the spectral matrix in momentum space is

$$\mathcal{H}(\mathbf{k})=\begin{pmatrix} g(\mathbf{k}) & if(\mathbf{k}) \\ -if^*(\mathbf{k}) & -g(\mathbf{k}) \end{pmatrix}, \tag{16}$$

where $f(\mathbf{k})=J_z+J_xe^{i\mathbf{k}\cdot\mathbf{n}_1}+J_2e^{i\mathbf{k}\cdot\mathbf{n}_2}$ and $g(\mathbf{k})=2K[\sin\mathbf{k}\cdot\mathbf{n}_1-\sin\mathbf{k}\cdot\mathbf{n}_2+\sin\mathbf{k}\cdot(\mathbf{n}_2-\mathbf{n}_1)]$ with $\mathbf{n}_1=(1,0)$ and $\mathbf{n}_2=(0,1)$. The system size is $N=2L^2$.

The inclusion of an external magnetic field gives rise to a transition between phases with Abelian and non-Abelian anyon excitations contained in the region $|J_z|\le|J_x|+|J_y|, |J_y|\le|J_z|+|J_x|, |J_x|\le|J_y|+|J_z|$ of the parameter

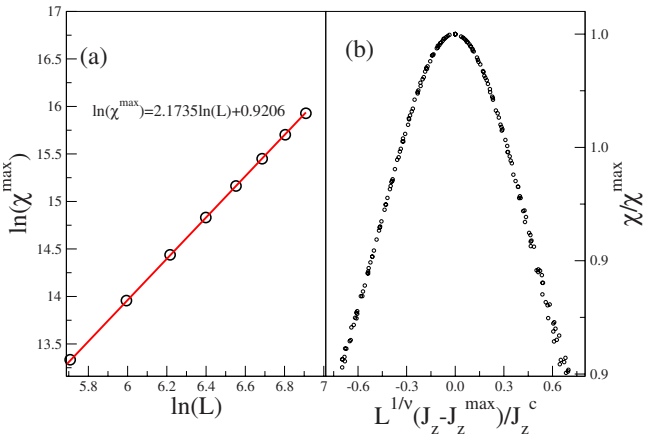


FIG. 6. (Color online) (a) Scaling analysis of the susceptibility for the Kitaev model with a weak Zeeman magnetic field at the critical point $J_z=1/2$. The system size range is $L\in[301,1001]$ in steps of 100 and the coupling $K=1/15$. The data imply that $\chi^{\max}/N\propto L^{\mu}$ with $\mu=0.1735\pm0.0001$ at criticality. (b) Data collapse of the fidelity susceptibility $\chi$ around the critical point $J_z^c=1/2$ $[J_x=J_y=0.5(1-J_z)]$ and $K=1/15$. We obtain $\nu=1.10\pm0.05$ for the critical exponent of the correlation length.

space. The numerical results for $\chi^{\max}/N\propto L^{\mu}$ for the honeycomb model with external magnetic field are shown in Fig. 6(a), where we obtain $\mu=0.1735\pm0.0001$, signaling superextensive scaling at criticality. The corresponding data collapse is shown in Fig. 6(b), with $\nu=1.10\pm0.05$ for the critical exponent of the correlation length, and $\alpha=\mu/\nu=0.158\pm0.007$.

For the models we have considered so far we see that the fidelity susceptibility is able to detect the phase transition between distinct topological phases, besides providing useful information about the critical point itself (i.e., the exponent $\nu$ of the correlation length).

### C. Three-dimensional model

The Hamiltonian in Eq. (3) has lines of zeros in momentum space with a vanishing gap. The addition of next-nearest-neighbor interactions that preserve time-reversal symmetry of the form

$$H^z_{\mathrm{nnn}}=i\sum_{jk}t^z(\lambda^4_j\lambda^4_k-\lambda^5_j\lambda^5_k), \tag{17}$$

$$H^x_{\mathrm{nnn}}=i\sum_{jk}t^x(\lambda^4_j\lambda^5_k+\lambda^5_j\lambda^4_k) \tag{18}$$

removes the degeneracy [11]. In momentum space the Hamiltonian (4) with the above perturbations can be written as

$$H=i\sum_{k}(a^4_{-k},a^5_{-k},b^4_{-k},b^5_{-k})\mathcal{H}(k)(a^4_k,a^5_k,b^4_k,b^5_k) \tag{19}$$

with $\mathcal{H}(k)$ given by

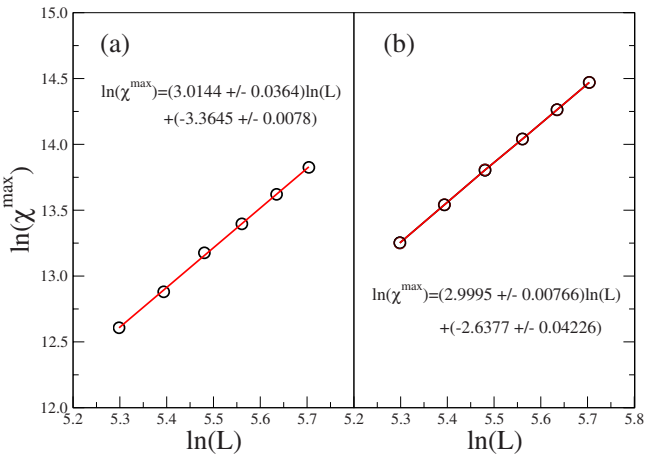


FIG. 7. (Color online) (a) Log-log plot of the fidelity susceptibility at the critical line for $\delta J_1=1$ and linear system size $L\in[200,300]$ in steps of 20. (b) Log-log plot of the fidelity susceptibility at the critical line for $t_z=0.1$ and linear system size $L\in[200,300]$ in steps of 20.

$$\mathcal{H}(\mathbf{k})=\begin{pmatrix}\Theta(\mathbf{k}) & i\Phi(\mathbf{k})\\ -i\Phi^*(\mathbf{k}) & -\Theta(\mathbf{k})\end{pmatrix}. \tag{20}$$

Defining the three-component vectors $s_0=\frac{1}{4}(-1,1,-1)$, $s_1=\frac{1}{4}(1,1,1)$, $s_2=\frac{1}{4}(-1,-1,1)$, and $s_3=\frac{1}{4}(1,-1,-1)$ (see Fig. 2), the blocks of matrix (20) are given by

$$\Phi(\mathbf{k})=\sum_{u=0}^{3}\sigma^0J_ue^{i\mathbf{k}\cdot s_u}, \tag{21}$$

$$\Theta(\mathbf{k})=\Theta^x(\mathbf{k})\sigma^x+\Theta^z(\mathbf{k})\sigma^z, \tag{22}$$

$$\Theta^x(\mathbf{k})=t^x\left[\sin\frac{k_x-k_y}{2}+\sin\frac{k_y-k_z}{2}+\sin\frac{k_z-k_x}{2}\right], \tag{23}$$

$$\Theta^z(\mathbf{k})=t^z\sin\frac{k_y+k_z}{2} \tag{24}$$

with $\sigma^0$ as the two-dimensional identity matrix and $\sigma^{x,z}$ as the usual Pauli matrices.

When all couplings $J$ are equal, there are still three degenerate points in the Brillouin zone at $(2\pi,0,0)$, $(0,2\pi,0)$, and $(0,0,2\pi)$. These degeneracies can be made massive by adding a small anisotropy in one of the couplings $J$. Following [11] we set $t^x=1$, $J_{2,3,4}=2$, and $J_1=2+\delta J_1$. The free parameters of the model are then $t^z$ and $\delta J_1$. The phase diagram presents three topologically distinct phases, distinguished by the winding number. For positive $\delta J_1$ and positive $t_z$ the winding number is +1; for positive $\delta J_1$ and negative $t_z$ the winding number is −1, and it is zero in the negative $\delta J_1$ region [11]. There are two topological phase transitions at the two critical lines $\delta J_1=0$ and $t_z=0$.

We have studied this model using the fidelity approach and in the following we present the results for the scaling of the fidelity susceptibility around the two phase transitions of the model. In Fig. 7(a) we show the log-log plot of the fidelity susceptibility at the $t_z=0$ critical line, while Fig. 7(b)

presents analogous results for the transition across the $\delta J_1=0$ line. In both cases the fidelity susceptibility has a peak at the critical point. The scaling analysis suggests that the fidelity susceptibility is extensive within the numerical precision that we could obtain from a first set of data. However, the numerical accuracy of this result cannot exclude a weak superextensive scaling at the critical point. A more accurate analysis of this model will be presented in a future work.

## IV. CONCLUSIONS

The fidelity approach proves to be a useful tool to detect and characterize quantum phase transitions which take place between distinct topological phases. We have applied it to the family of mosaic models which presents a transition between topological phases with Abelian and non-Abelian anyons, as well as the Kitaev model with an external magnetic field, where a transition from an Abelian to a non-Abelian phase takes place. We were able to show superextensive scaling of the fidelity susceptibility at criticality, characterizing its behavior in the thermodynamic limit. We also extracted the critical exponent of the correlation length for these models. Moreover, we studied the transition between a topological insulator and a topological superconductor in a three-dimensional diamond lattice, where the method still detects the boundary between different phases. In this case, superextensivity of the fidelity susceptibility turns out to be more difficult to be established. This is probably due to the increased dimensionality which weakens the features of the quantum phase transitions.

We have thus extended the applicability of the fidelity approach to the boundary that separates different topological phases and proved its usefulness in this context as well. Since it is not always clear how to detect and distinguish different topological phases of matter we believe that it is important to check the validity of a method based solely on the geometrical properties of the ground state, and that does not require the introduction of an order parameter.

## ACKNOWLEDGMENTS

We thank K. Shtengel for pointing us Ref. [6] and H. Yao for helpful discussions. Computation for the work described in this paper was supported by the University of Southern California Center for High Performance Computing and Communications. We acknowledge financial support by the National Science Foundation under Grant No. DMR-0804914.

[1] X.-G. Wen, Int. J. Mod. Phys. B **4**, 239 (1990); X.-G. Wen and Q. Niu, Phys. Rev. B **41**, 9377 (1990); X.-G. Wen, Phys. Rev. B **44**, 2664 (1991).
[2] N. Read and S. Sachdev, Phys. Rev. Lett. **66**, 1773 (1991).
[3] A. Y. Kitaev, Ann. Phys. (N.Y.) **321**, 2 (2006).
[4] D. J. Thouless, M. Kohmoto, M. P. Nightingale, and M. den Nijs, Phys. Rev. Lett. **49**, 405 (1982).
[5] C. L. Kane and E. J. Mele, Phys. Rev. Lett. **95**, 146802 (2005).
[6] H. Yao and S. A. Kivelson, Phys. Rev. Lett. **99**, 247203 (2007).
[7] B. A. Bernevig, T. L. Hughes, and S. Zhang, Science **314**, 1757 (2006).
[8] C. Nayak, S. H. Simon, A. Stern, M. Freedman, and S. Das Sarma, Rev. Mod. Phys. **80**, 1083 (2008).
[9] J. K. Pachos, Ann. Phys. **322**, 1254 (2006).
[10] J. Vidal, K. P. Schmidt, and S. Dusuel, Phys. Rev. B **78**, 245121 (2008).
[11] S. Ryu, e-print arXiv:0811.2036.
[12] S. Yang, D. L. Zhou, and C. P. Sun, Phys. Rev. B **76**, 180404(R) (2007).
[13] L. Amico, R. Fazio, A. Osterloh, and V. Vedral, Rev. Mod. Phys. **80**, 517 (2008).
[14] P. Zanardi and N. Paunković, Phys. Rev. E **74**, 031123 (2006).
[15] H.-Q. Zhou and J. P. Barjaktarevič, e-print arXiv:cond-mat/0701608; H.-Q. Zhou, J.-H. Zhao, and B. Li, e-print arXiv:0704.2940; H.-Q. Zhou, e-print arXiv:0704.2945.
[16] P. Zanardi, P. Giorda, and M. Cozzini, Phys. Rev. Lett. **99**, 100603 (2007).
[17] P. Zanardi, M. Cozzini, and P. Giorda, J. Stat. Mech.: Theory Exp. **2007**, L02002.
[18] L. Campos Venuti and P. Zanardi, Phys. Rev. Lett. **99**, 095701 (2007).
[19] S.-J. Gu, e-print arXiv:0811.3127.
[20] A. Hamma, W. Zhang, S. Haas, and D. A. Lidar, Phys. Rev. B **77**, 155111 (2008).
[21] D. F. Abasto and P. Zanardi, Phys. Rev. A **79**, 012321 (2009).
[22] D. F. Abasto, A. Hamma, and P. Zanardi, Phys. Rev. A **78**, 010301(R) (2008).
[23] S. Yang, S.-J. Gu, C.-P. Sun, and H.-Q. Lin, Phys. Rev. A **78**, 012304 (2008).
[24] J.-H. Zhao and H.-Q. Zhou, e-print arXiv:0803.0814.
[25] W.-L. You, Y.-W. Li, and S.-J. Gu, Phys. Rev. E **76**, 022101 (2007).
[26] E. H. Lieb, Phys. Rev. Lett. **73**, 2158 (1994).
[27] V. Lahtinen, G. Kells, A. Carollo, T. Stitt, J. Vala, and J. K. Pachos, Ann. Phys. (N.Y.) **323**, 2286 (2008).
[28] C. Wu, D. Arovas, and H.-H. Hung, e-print arXiv:0811.1380.
[29] J. C. Slater, *Quantum Theory of Atomic Structure* (McGraw-Hill, London, 1960), Vol. 1, p. 291.
[30] S. Yang, D. L. Zhou, and C. P. Sun, Phys. Rev. B **76**, 180404(R) (2007).
[31] S. Dusuel, K. P. Schmidt, J. Vidal, and R. L. Zaffino, Phys. Rev. B **78**, 125102 (2008).
[32] J. G. Brankov, D. M. Danchev, and N. S. Tonchev, *Theory of Critical Phenomena in Finite-Size Systems* (World Scientific, Singapore, 2000).
[33] S. M. Bhattacharjee and F. Seno, J. Phys. A **34**, 6375 (2001).